

HIGH-FREQUENCY STABILIZATION OF THE KADOMTSEV-NEDOPASOV INSTABILITY IN AN ELECTRON-HOLE PLASMA

V. V. VLADIMIROV, L. V. DUBOVOÏ and V. F. SHANSKIÏ

D. V. Efremov Institute for Electro-physical Apparatus

Submitted November 17, 1969

Zh. Eksp. Teor. Fiz. 58, 1580–1585 (May, 1970)

Conditions are derived for the high-frequency stabilization of the helical instability associated with a current flow in the electron-hole plasma in a semiconductor. The results of the calculations are compared with the experimental data for germanium. It is shown that the model used in the calculations explains the basic experimental features.

IN recent years a great deal of interest has been focused on the interaction of high-frequency electromagnetic fields and a plasma in an unstable state. The potential usefulness of work in this direction is due, in particular, to the hope of realizing conditions under which the externally produced high-frequency fields in a plasma can bring about stabilization of certain kinds of MHD instabilities. The present work is devoted to an investigation of high-frequency stabilization of the helical instability associated with current flow in the electron-hole plasma in a semiconductor. At the present time this instability represents one of the most frequently encountered in the field. This instability was first observed in a semiconductor plasma in experiments reported by Ivanov and Ryvkin^[1]; a complete theory of the effect was developed by Glicksman^[2] on the basis of a model proposed earlier by Kadomtsev and Nedopasov^[3] in the analysis of the plasma in the positive column of a gas discharge.

The stabilization of the helical instability driven by a current in an electron-hole plasma in germanium was observed and explained by the authors of the present work^[4-6] together with Kadomtsev. Calculations^[5] have shown that to explain high-frequency stabilization it is necessary to supplement the analysis in^[2] by the introduction of boundary conditions at the end faces; these conditions require nodes in the perturbation currents at the end faces. The solution appears in the form of a superposition of standing waves. The behavior of the system is then described by the Hill equation and high-frequency stabilization of the current perturbations corresponds to operation in the stability regions of this equation. In this model the stabilization effect is due to the time-correlation between space harmonics with different wave number n . In what follows the efficiency of the process will be characterized by a modulation coefficient $\eta_c = \tilde{E}/E_c$ where E_c is the electric field that drives the instability^[2] and \tilde{E} is the alternating component of the field E_c that causes a reduction of the amplitude of the current perturbation by a factor of e .

In the present work, taking account of the two most dangerous longwave unstable modes, characterized by $n = 1$ and $n = 2$, we extend the results of the calculation in^[5]; we find the dependence of η_c on the length of the sample for various modulation frequencies and determine the limiting values of the fixed electric and mag-

netic fields for which high-frequency stabilization is possible. The results of the calculation are compared with the experimental data. The calculation and the experiment pertain to the case of an unmagnetized plasma which satisfies the condition $\omega_c \tau \ll 1$ where ω_c and τ are respectively the cyclotron frequency and the momentum relaxation time for the current carriers.

If $\omega_c \tau \ll 1$ the basic equation that describes the helical instability is^[5]

$$\hat{L}n' = \frac{\partial^4 n'}{\partial x^4} - n',$$

where

$$\hat{L} = \frac{\partial}{\partial t} \left(\frac{\partial^2}{\partial x^2} - 1 \right) + 2 \left(\frac{\partial^2}{\partial x^2} - 1 \right) - i\alpha(1 + \eta \sin \beta\theta) \frac{\partial}{\partial x}.$$

Here

$$\theta = \frac{D_e}{a^2(1+b)}t, \quad \alpha = \frac{0,16\omega_c\tau_n(1+b)u_{0e}a}{D_e},$$

$$\beta = \frac{\omega_0(1+b)a^2}{D_e}, \quad x = 0,5 \frac{z}{a},$$

and z is the running coordinate in the direction of the sample axis, a is the radius of the sample, t is the time, D_e is the electron diffusion coefficient, b is the ratio of the mobilities of the electrons and holes, and ω_0 is the modulation frequency of the electric field. In order-of-magnitude terms β is the same as the ratio of the modulation frequency to the instability frequency. Expressions for the dimensionless quantities are given for the case of a clean surface in which the parameter $G = 2D_e/(1+b)as \approx 25$ where s is the surface recombination rate. The experimental situation approximates the case of a clean surface and the measurements are carried out with Ge samples with a natural conductivity for several doping levels. Under these conditions it can be assumed that the stationary distribution of carriers is uniform over the cross section of the sample.

In the case of weakly injected contacts the boundary conditions for the end faces are

$$n' |_{x=0,x_L} = 0, \tag{2}$$

where $x_L = 0.5 L/a$. The choice of zero boundary conditions or nodes at the ends is verified by the experimental data.^[6]

A solution of Eq. (1) in the form of plane waves $\exp(ikz)$ does not satisfy the boundary condition in Eq.

(2).^[2] Since the variables do not separate in Eq. (1), the solution of Eq. (1) is sought in the form of an expansion in characteristic coordinate functions Φ_n of the operator L which satisfy the boundary conditions in (2):

$$n' = \sum_n c_n(\theta) \Phi_n(x), \quad (3)$$

where

$$\Phi_n(x) = \exp\{i\rho_n x\} \sin \kappa_n x, \quad \rho_n = \sqrt{1 + \kappa_n^2}, \\ \kappa_n = \pi n / x_L, \quad n = 1, 2, 3 \dots$$

This approach to the solution of Eq. (1) is essentially a perturbation method; the right side of Eq. (1) is a quantity of order a/L when the solution in the form of (3) is substituted, and is small in long samples.

The subsequent analysis is carried out in a two-mode approximation. Forming a system of functions which are orthogonal to Φ_1 and Φ_2 in accordance with^[5] and averaging over the coordinate x (Kantorovich method) we convert Eq. (1), a partial differential equation, into a system of two ordinary first-order differential equations in the functions $c_1(\theta)$ and $c_2(\theta)$. Solving this system with respect to each of the functions c_1 and c_2 we obtain a second-order equation of the form

$$\ddot{c}_1 + 2\epsilon \dot{c}_1 + \kappa c_1 = 0. \quad (4)$$

The expressions for the coefficients ϵ and κ are

$$\epsilon = 2(\rho_1^2 + \rho_2^2) - \frac{2}{\mathcal{L}} - \frac{\alpha}{4} \left(\frac{1}{\rho_1} + \frac{1}{\rho_2} \right) (1 + \eta \sin \beta\theta), \\ \kappa = \left[4\rho_1^2 - \frac{\alpha}{2\rho_1} (1 + \eta \sin \beta\theta) \right] \left[4\rho_2^2 - \frac{\alpha}{2\rho_2} (1 + \eta \sin \beta\theta) \right] \\ - \frac{4}{\mathcal{L}} \left[4\rho_1\rho_2 - \frac{4\rho_1\rho_2}{(\rho_1 + \rho_2)^2} - \frac{\alpha}{2} \frac{\rho_1^2 + \rho_2^2}{\rho_1\rho_2(\rho_1 + \rho_2)} (1 + \eta \sin \beta\theta) \right] \\ - \frac{\alpha}{2\rho_1} \beta\eta \cos \beta\theta;$$

where

$$\mathcal{L} = 1 - 2 \left(\frac{8}{3} \right)^2 \left(\frac{\rho_2 - \rho_1}{\rho_1 + \rho_2} \right)^2 \frac{1}{1 + \cos(\rho_2 + \rho_1)x_L}.$$

The solution of Eq. (4) can be written conveniently in the form

$$c_1 = \text{const} \cdot \exp \left(- \int \epsilon d\theta \right) u(\theta),$$

where $u(\theta)$ satisfies the equation

$$\ddot{u} + (\kappa - \epsilon^2 - \dot{\epsilon})u = 0. \quad (5)$$

The high-frequency stabilization effect can be realized when the development of the instability is determined by Eq. (5) in the absence of the high-frequency field, or when

$$\epsilon(\eta=0) > 0, \quad \kappa(\eta=0) < 0. \quad (6)$$

The condition in (6) indicates the range of values of α for which high-frequency stabilization is possible:

$$\alpha_{\min} \leq \alpha \leq \alpha_{\max}. \quad (7)$$

Here, α_{\min} and α_{\max} are given by the following expressions:

$$\alpha_{\min} = 4(\rho_1 + \rho_2)(\rho_1^2 - \rho_1\rho_2 + \rho_2^2) - \frac{4}{\mathcal{L}} \frac{\rho_1^2 + \rho_2^2}{\rho_1 + \rho_2} - 4(\rho_2 - \rho_1) \\ \times \left\{ (\rho_1^2 + \rho_1\rho_2 + \rho_2^2) \left(\rho_1^2 + \rho_1\rho_2 + \rho_2^2 - \frac{2}{\mathcal{L}} \right) \right.$$

$$\left. + \frac{1}{\mathcal{L}^2} \left[1 + \frac{8(8/3)^2 \rho_1^2 \rho_2^2}{(\rho_1 + \rho_2)^4} \frac{1}{1 - \cos(\rho_2 - \rho_1)x_L} \right] \right\}^{1/2}, \\ \alpha_{\max} = \frac{8\rho_1\rho_2}{\rho_1 + \rho_2} \left(\rho_1^2 + \rho_2^2 - \frac{1}{\mathcal{L}} \right).$$

Equation (5), which governs the function u , is in the form of a generalized Hill equation.^[5] In this case, the criteria which determine the region of stable behavior of the system for low characteristic frequencies reduce to an equation for stabilizing values of η_c :

$$\eta_c^4 + p\eta_c^2 - q \geq 0. \quad (8)$$

The expressions for p and q which appear in Eq. (8) can be written conveniently in the form

$$p = \frac{16^3 \rho_1^2 \rho_2^2}{\alpha^2} \left[\rho_1 + \rho_2 + \frac{\alpha_1}{8\rho_1\rho_2} - \frac{1}{\mathcal{L}(\rho_1 + \rho_2)} \right]^2; \\ q = \frac{8 \cdot 16^3 \rho_1^4 \rho_2^4}{\alpha^4 (\rho_2 - \rho_1)^2} \left\{ \left[\rho_1 + \rho_2 + \frac{\alpha}{8\rho_1\rho_2} \right]^2 + \frac{1}{\mathcal{L}} \left[\frac{1}{\mathcal{L}(\rho_1 + \rho_2)^2} \right. \right. \\ \left. \left. + \frac{8(8/3)^2 \rho_1 \rho_2}{\mathcal{L}(\rho_1 + \rho_2)^4 [1 - \cos(\rho_2 - \rho_1)x_L]} - 2 - \frac{\alpha}{4\rho_1\rho_2(\rho_1 + \rho_2)} \right] \right\} \beta^2.$$

If the sample is not too long ($L/a \lesssim 25$) it follows from Eq. (8) that $\eta_c \approx \sqrt{\omega_0} L/a$. The physical meaning of this relation can be understood easily because an increase in the modulation frequency implies that the correction due to the high-frequency field in the average equation (5) falls off with time (a similar situation arises in the dynamic stabilization of the inverted pendulum^[7]) while the correlation between modes is reduced with increasing sample length.^[5]

The results of calculations of the actual values of $\eta_c(L/a)$ obtained for the lower boundary of the high-frequency stabilization region $\alpha \approx \alpha_{\min}$ and the relation with the experimental data are discussed in detail below.

In an experimental test of this analysis use has been made of germanium with a value of conductivity close to the natural value ($\rho_0 = 45 \text{ ohm} \cdot \text{cm}$). Samples with weakly injected tin contacts having transverse dimensions $1 \times 1 \text{ mm}$ and a length varying from 3 to 15 mm were used. The method of determining the time in which the instability grows is similar to that used in^[4]. In the experiments we detect oscillations in the potential with point probes located at the side surfaces of the samples. The length of the electric field pulse $E_c = 100 \text{ } \mu\text{sec}$ and the length of the high-frequency field pulse \tilde{E} is of the order of $50 \text{ } \mu\text{sec}$. Pulsed operation is used in order to avoid heating of the lattice by current flow.

The modulation frequency for the electric field \tilde{E} is $\omega_0 = 6 \times 10^6 \text{ Hz}$; since the frequency of the oscillations associated with the instability $\omega \approx 1 \times 10^5 \text{ Hz}$, the inequality $\omega_0/\omega \sim 10 \gg 1$ is always satisfied.

The magnetic field in the experiments can be varied from 0 to 12 kG. In order to avoid overheating of the current carriers the instability is excited by varying the magnetic field with a relatively weak fixed value of the field $E_c = 100 \text{ V/cm}$.

In Fig. 1 we show the stability boundary for high-frequency stabilization computed in the two-mode approximation together with the results of the corresponding measurements. The boundaries of the region corresponding to the minimum values of $\alpha_{\min}(L/a)$ coincide with the threshold values $\alpha_c \sim B_c$ for excitation of the

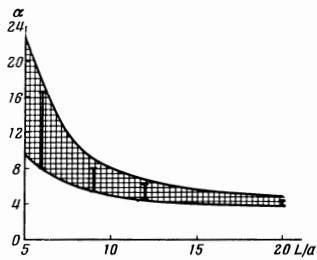


FIG. 1. Boundaries of the zone of high-frequency stabilization. The region in which high-frequency fields can be used for suppression of the instability is shown in cross hatching. The vertical lines show the results of the measurements of various values of L/a .

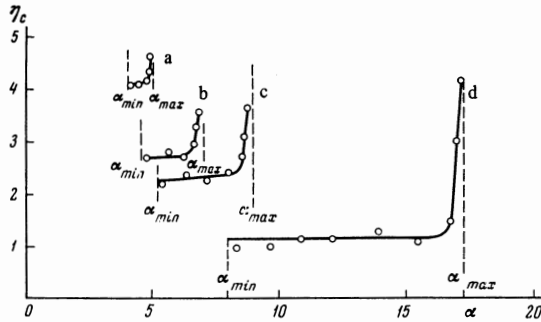


FIG. 2. Results of the measurements of the function $\eta_c(\alpha)$ for various L/a : a) $L/a = 20$, b) $L/a = 12$, c) $L/a = 9$, d) $L/a = 6$. The quantities α_{\min} and α_{\max} are the smallest and largest values of α for which high-frequency stabilization is realized for finite η_c ; $E_c = \text{const}$.

helical instability in samples with various values of L/a .

In Fig. 2 we show the experimentally measured functional relation $\eta_c(\alpha)$ for various values of L/a . The calculated positions of the stability boundaries in Fig. 2 are denoted by dashed lines for the corresponding values of α_{\min} and α_{\max} . It is evident that as α increases the quantity η_c first remains constant and then rises sharply. The values of α for which there is a sharp rise in η_c can be identified with the upper boundary of the largest values of α ; beyond this boundary the stabilizing effect does not operate.

For purposes of comparison the experimentally determined stability zones for various sample lengths are shown in Fig. 1 as solid vertical lines. As is evident from Figs. 1 and 2, the calculated position of the boundaries of the zone expected for high-frequency stabilization are in satisfactory agreement with the experimental data. An unexpected effect is the sharp increase in the stabilizing value of the modulation coefficient η_c close to the upper limit of the zone beyond which the high-frequency stabilization effect no longer appears. This effect is evidently a natural consequence of the transition from the region of stable behavior of the system into the unstable region.

In Fig. 3 we show experimental values of η_c and calculated values for $\beta = 10$ and $\beta = 20$ for $\alpha = \alpha_{\min}$ as a function of sample length L . It is evident that the stabilizing value increases with increasing L and that this relation is essentially linear; however, the calculated values of η_c are two or three times greater than the measured values. At the present time we can indicate two possible reasons for this discrepancy between the calculations and the experimental data shown in Fig. 3. The first is the approximate nature of the calculations; this arises from the fact that in our method of determining η_c we only consider the two longest wavelength

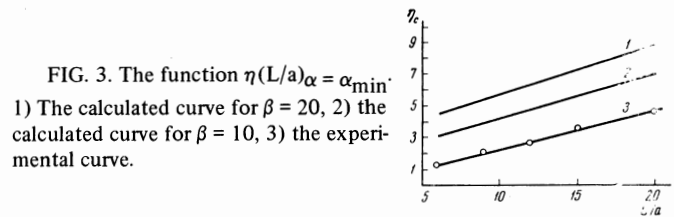


FIG. 3. The function $\eta_c(L/a)\alpha = \alpha_{\min}$. 1) The calculated curve for $\beta = 20$, 2) the calculated curve for $\beta = 10$, 3) the experimental curve.

modes of the instability. Actually, when $\alpha > \alpha_{\min}$ the experiments always exhibit a wide spectrum of modes, with space harmonics extending up to the fifth and higher.^[6] At the same time as is indicated by experiment^[4-6], the appearance of a large number of higher order space harmonics is always accompanied by a reduction in η_c .

Another possible cause for the difference that has been observed may be the use of the classical diffusion coefficient D_e in the calculation in place of an effective coefficient D_{eff} due to plasma turbulence when $\alpha > \alpha_{\min}$. Thus the discrepancy between the calculated and observed values can be reduced significantly if use is made of the empirical value $D_{\text{eff}} \approx (3-6)D_e$, which is obtained by measurements of the profile of the plasma density in the semiconductor.

Unfortunately, any attempt to carry out a rigorous calculation of $\eta_c(\alpha)$ taking account of the large number of space harmonics and the effective diffusion coefficient D_{eff} involves a number of serious technical difficulties; as the number of modes included in the calculation increases the order of the basic differential equation increases and, in turn, this leads to the need for machine calculations.

In concluding the discussion of the results that have been obtained we note that in spite of certain discrepancies between the experimental data and the calculations there is satisfactory qualitative agreement. Even with the two-mode approximation the model developed here for the investigation of high-frequency stabilization of the helical instability due to current flow in a semiconductor plasma is completely adequate for the description of the basic features of the experimental results when $\omega_c \tau \ll 1$.

It would be of great interest to investigate high-frequency stabilization of the helical instability in a strong magnetic field in which $\omega_c \tau \gg 1$.

The authors are highly indebted to B. B. Kadomtsev for useful discussions of the work.

¹ Yu. L. Ivanov and S. M. Ryvkin, Zh. Tekh. Fiz. 28, 774 (1958) [Sov. Phys.-Tech. Phys. 3, 722 (1958)].

² M. Glicksman, Phys. Rev. 124, 1655 (1961).

³ B. B. Kadomtsev and A. V. Nedospasov, J. Nuclear Energy, Part C, 1, 230 (1960).

⁴ L. V. DubovoĀ and V. F. ShanskiĀ, Zh. Eksp. Teor. Fiz. 48, 800 (1965) [Sov. Phys.-JETP 21, 530 (1965)].

⁵ V. V. Vladimirov, Zh. Eksp. Teor. Fiz. 49, 1526 (1965) [Sov. Phys.-JETP 22, 1047 (1966)].

⁶ L. V. DubovoĀ and V. F. ShanskiĀ, Zh. Eksp. Teor. Fiz. 51, 412 (1966) [Sov. Phys.-JETP 24, 276 (1967)].

⁷ P. L. Kapitza, Zh. Eksp. Teor. Fiz. 21, 588 (1951).